[7]Cooke, C. H., and Fansler, K. S., "Comparison with Experiment for TVD Calculations of Blast Waves from a Shock Tube," *International Journal for Numerical Methods in Fluids*, Vol. 9, No. 1, 1989, pp. 9–22.

Turbulent Flow Measurements with a Triple-Split Hot-Film Probe

M. D. Doiron* and D. W. Zingg†
University of Toronto, Toronto, Ontario M3H 5T6, Canada

Nomenclature

A_{jk}	= asymmetry correction factor
$a_0,\ldots,a_3$	= polynomial coefficients for velocity magnitude
$b_{i,0},\ldots,b_{i,6}$	= Fourier series coefficients for velocity direction, $i = 1, 2, 3$
$c_{i,j,0},\ldots,c_{i,j,3}$	= polynomial coefficients for velocity direction Fourier series coefficients, $i = 1, 2, 3$ and $j = 0, 1,\ldots,6$
$d_0,\ldots,d_{10}$	= Fourier series coefficients for correction factor
E_i	= output voltage for individual sensor, $i = 1, 2, 3$
$e_{k,0},\ldots,e_{k,2}$	= polynomial coefficient for correction factor Fourier series coefficients, $k = 0, 1,\ldots,10$
U	= velocity magnitude
α	= angle of attack
ΣE_i^2	= sum of the squares of the sensor voltages
Θ	= azimuthal or flow angle

Introduction

COMPLEX turbulent shear flows occur in many aerospace applications, such as aerodynamic devices and gas turbine engines. Measurements of mean and fluctuating velocity components can greatly aid our understanding of such flows. Experimental data are particularly useful in assessing and validating turbulence models used in computational fluid dynamics codes. Velocity measurements are generally made using a pitot-static tube, a constant temperature hot-wire anemometer, or a laser Doppler anemometer (LDA). For separated turbulent flows, pitot-static tubes and conventional hot-wire probes are generally inapplicable.[1] Because of the high cost of LDA measurements, modified hot-wire techniques have been developed which are suitable for reversed flows. These include pulsed hot wires[2] and flying hot wires.[3] Disadvantages of these approaches are discussed by Nakayama.[4]

Triple-split hot-film probes are a potentially useful alternative for velocity measurements in separated turbulent flows. Such probes typically consist of three separate films deposited on a cylinder. The operating principle is based on the variation of the local heat transfer coefficient on a cylinder with the magnitude and direction of the oncoming flow velocity. Most studies involving split-film anemometry have been with double-split hot-film probes. These operate on the same principle but retain the directional ambiguity of conventional hot wires and, hence, are not applicable to separated turbulent flows. The results of these studies indicate that split-film probes provide comparable accuracy to hot-wire probes for mean velocities but have a more limited frequency response.[4] Despite their potential, especially for measurements of mean velocities, triple-split hot-film probes have received little use. The only example of their use known to the authors is reported by Modera,[5] who used a triple-split probe for low-frequency reversed flow measurements over a 0–8 m/s flow speed range. The purpose of this Note is to demonstrate that the triple-split hot-film probe can be very useful for measurements of mean velocities in separated turbulent flows. Further details of the present study are given in Ref. 6.

Received June 28, 1993; revision received April 14, 1994; accepted for publication April 19, 1994.

*Research Assistant, Institute for Aerospace Studies, 4925 Dufferin St.
†Assistant Professor, Institute for Aerospace Studies, 4925 Dufferin St. Member AIAA.

Calibration Procedure

The triple-split hot-film probe used (Dantec model 55R94) consists of three nickel films deposited on a 400-μm-diam quartz cylinder, with each film occupying approximately 120 deg of the circumference as shown in Fig. 1. As such, the probe can resolve two-dimensional velocity components in a plane perpendicular to the axis of the probe for any flow angle Θ through a full 360 deg. The calibration procedure is described in detail in Ref. 6. It is largely based on the method of Jørgensen,[7] with an extension to account for asymmetries in the characteristics of the probe. A calibration rig that is capable of providing a range of known flow speeds and flow angles, through 360 deg, is necessary for the calibration.

With a perfectly symmetric probe, the calibration scheme could allow for independent determination of the magnitude and direction of the velocity. However, actual probes can have asymmetries resulting from mismatched films, imbalances in film temperatures and sensitivities, and probe body effects. These effects generally couple the determination of the velocity magnitude and direction. Expressions will first be given that assume the independence of the magnitude and direction. A correction factor will then be incorporated that couples magnitude and direction determination through an iterative procedure. All curve fits were performed using the least squares method.

The calibration is carried out at a number of flow speeds, typically 6, spanning the range of foreseeable test speeds. For each given calibration speed, the calibration is performed at a number of flow angles, typically 18, evenly spaced through the full 360 deg. The sum of the squares of the sensor voltages ΣE_i^2 is a measure of the total heat convected from the probe and is ideally not influenced by flow direction. This initial assumption is important since the average value of ΣE_i^2 over all flow angles for a given flow speed was used for calibration purposes. The velocity magnitude is determined from the following third-order polynomial in ΣE_i^2,

$$U = a_0 + a_1(\Sigma E_i^2) + a_2(\Sigma E_i^2)^2 + a_3(\Sigma E_i^2)^3 \tag{1}$$

The velocity direction is determined by modeling the angular response of each of the three sensors by a third-order Fourier series, as follows.

$$E_i(U,\Theta) = b_{i,0} + b_{i,1}\cos\Theta + b_{i,2}\cos 2\Theta + b_{i,3}\cos 3\Theta + b_{i,4}\sin\Theta + b_{i,5}\sin 2\Theta + b_{i,6}\sin 3\Theta \tag{2}$$

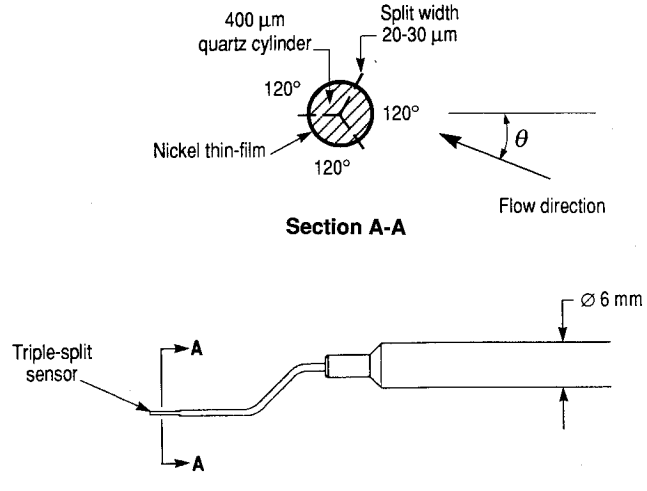

Fig. 1 Triple-split hot-film probe.

Table 1 Typical velocity magnitude errors for a velocity of 46.3 m/s with and without the asymmetry correction

Quantity	Uncorrected, m/s	Corrected, m/s
Average error	4.3	0.6
Maximum negative error	−7.5	−1.5
Maximum positive error	4.4	0.5
standard deviation	2.1	0.5

for $i = 1, 2, 3$. In Eq. (2), the Fourier coefficients $b_{i,0}, \ldots, b_{i,6}$ for each sensor are first determined for each of the calibration speeds, with E_i and Θ known. Since these coefficients are themselves a function of the flow magnitude, represented by E_i^2, each is in turn modeled by a polynomial of the form given in Eq. (3). Note that the angular response modeling is done using two levels of curve fits. Specifically, the coefficients first determined through Eq. (2) are only used to provide $b_{i,j}$ values for Eq. (3) and are then discarded.

$$b_{i,j} = c_{i,j,0} + c_{i,j,1}(\Sigma E_i^2) + c_{i,j,2}(\Sigma E_i^2)^2 + c_{i,j,3}(\Sigma E_i^2)^3 \quad (3)$$

for $i = 1, 2, 3$ and $j = 0, 1, 2, \ldots, 6$. Equations (1–3) would be sufficient if the determination of velocity magnitude and direction were independent. Note that so far 88 calibration coefficients (four for magnitude $a_0, \ldots, a_3$, and $3 \times 7 \times 4 = 84$ for direction $c_{i,j,0}, \ldots, c_{i,j,3}$) are required. Once the calibration coefficients are found, use of these equations to calculate velocity components from measured experimental sensor voltages would proceed as follows. First, the velocity magnitude is easily found from Eq. (1). Next, Eq. (3) is used to calculate the Fourier coefficients $b_{i,j}$. Given the experimental sensor voltages and the Fourier coefficients, a search routine can be utilized with Eq. (2) to calculate the experimental flow direction Θ.

As a result primarily of the effect of the probe body on the flow, the total heat transfer from the probe ΣE_i^2 is a relatively strong function of the flow direction. In other words, at a given flow magnitude U the sum of the squared voltages varies with Θ. As stated earlier, the determination of the calibration coefficients in Eqs. (1–3) used an average value of ΣE_i^2 over all calibration flow angles. Since the flow angle associated with an experimental value of ΣE_i^2 would be as yet unknown, a correction to ΣE_i^2 must be applied to give an equivalent average value to achieve accuracy. Without such a correction, the films would have to be very closely matched, and probe body effects would have to be negligible. Based on their work with double-split probes, Shook et al.[8] reported that it is often not possible to adjust the films to achieve acceptable matching, probably due to manufacturing inconsistencies. The correction factor is defined as

$$A_{jk} \equiv \frac{(\Sigma E_i^2)_{\text{corrected}}}{(\Sigma E_i^2)_{\text{uncorrected}}} = \frac{(\overline{\Sigma E_i^2})_j}{(\Sigma E_i^2)_{jk}} \quad (4)$$

for $j = 1, 2, \ldots,$ number of calibration speeds and $k = 1, 2, \ldots,$ number of calibration angles. The overbar in this equation denotes the average value over all calibration flow angles at a given flow speed and is the value used in the curve-fits of Eqs. (1–3). The uncorrected value refers to measured experimental sensor voltages. The correction factors are modeled using a fifth-order Fourier series. As for Eqs. (2) and (3), these Fourier coefficients are also functions of flow magnitude and are in turn curve fitted to quadratic polynomials in ΣE_i^2. Hence, the correction factor is a function of both the flow direction and the flow speed, as follows:

$$A(U, \theta) = d_0 + d_1 \cos\theta + \cdots + d_5 \cos 5\theta + d_6 \sin\theta + \cdots + d_{10} \sin 5\theta \quad (5)$$

$$d_k = e_{k,0} + e_{k,1}(\Sigma E_i^2) + e_{k,2}(\Sigma E_i^2)^2 \quad (6)$$

for $k = 0, 1, 2, \ldots, 10$. Note that the determination of the correction factors through Eqs. (5) and (6) is independent of Eqs. (1–3). These factors are only used to correct the value of the sum of the squared voltages. The asymmetry correction adds $11 \times 3 = 33$ calibration constants to the 88 previously required for a total of 121 calibration constants. Once all of these constants have been calculated, the determination of experimental velocity components, with asymmetry correction, is accomplished as follows.

1) Measured experimental values of E_i, expressed as ΣE_i^2, are used in Eq. (1) to calculate velocity magnitude U.

2) The same ΣE_i^2 value is used in Eq. (3) to calculate the Fourier coefficients of Eq. (2).

3) Eq. (2) is solved, using a search routine, for the velocity direction Θ.

4) The current ΣE_i^2 value is used in Eq. (6) to determine the Fourier coefficients of Eq. (5).

5) The direction Θ found in step (3) is used to calculate the correction factor using Eq. (5).

6) The current value ΣE_i^2 is multiplied by the correction factor found in step (5).

7) Steps (1–6) are repeated with corrected values of ΣE_i^2 until converged values of U and Θ are achieved.

Two to four iterative cycles were typically required, depending on the degree of accuracy desired. Angular response curves for a typical calibration are given in Fig. 2 for three calibration speeds. The symbols indicate measured values whereas the curves represent the Fourier series fits. The unmatched operating characteris-

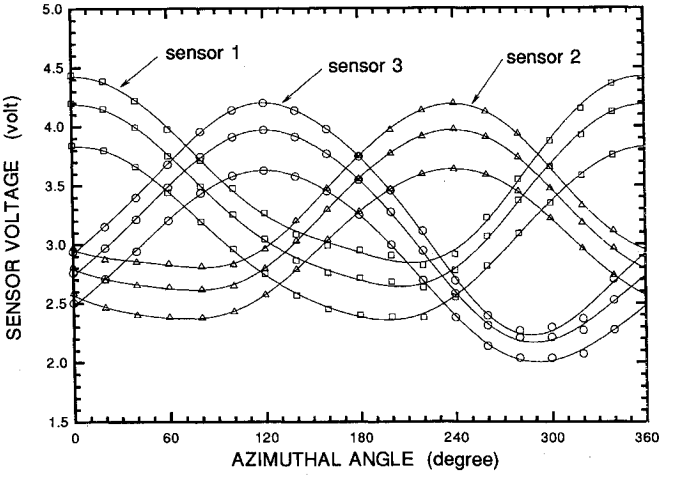

Fig. 2 Typical angular response curves for three calibration velocities.

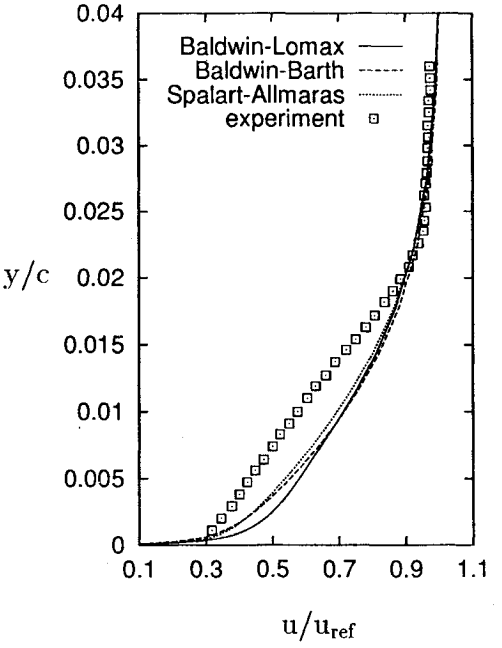

Fig. 3 Mean velocity profiles, $\alpha = 0$ deg, $x/c = 0.960$.

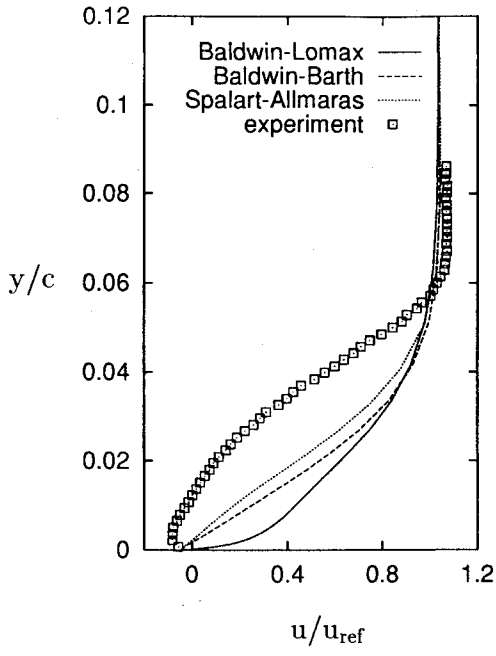

Fig. 4 Mean velocity profiles, $\alpha = 9.2$ deg, $x/c = 0.950$.

tics of the three films are evident. The improvements in the velocity magnitude errors resulting from the asymmetry correction for a typical calibration are shown in Table 1.

Results

The triple-split hot-film probe was used to measure mean velocities near the trailing edge of a 17% thick airfoil with moderate aft loading at two angles of attack, $\alpha = 0$ and $\alpha = 9.2$ deg. At $\alpha = 0$ deg, the flow is fully attached, whereas at $\alpha = 9.2$ deg there is a region of separated flow extending over approximately 20% chord. The tests were run at a chord-based Reynolds number of roughly 1.7×10^6 and a Mach number of 0.15. Transition was fixed at 8% chord on both surfaces, although it undoubtedly occurs earlier on the upper surface at the higher angle of attack.

Figure 3 shows the measured mean velocity profile in the boundary layer on the upper surface of the airfoil at $\alpha = 0$ deg. Also shown are computational results obtained using the well-established Navier-Stokes code ARC2D[9] with three different turbulence models, the Baldwin-Lomax model, the Baldwin-Barth model, and the Spalart-Allmaras model. Agreement between the measured and computed values is quite typical of attached adverse pressure gradient flows. Similar results for $\alpha = 9.2$ deg are shown in Fig. 4. The computed results drastically underestimate the thickness of the separated region. This is also typical for this flow solver, as discussed, for example, by Nelson et al.[10]

Conclusions

The calibration procedure for triple-split hot-film probes has been extended for probe asymmetry effects, leading to a substantial reduction in velocity magnitude errors. The probe has been used to measure mean velocity components in attached and separated two-dimensional turbulent flows about an airfoil. The results are sufficiently promising to justify further investigation of the probe.

References

[1]Simpson, R. L., "Two-Dimensional Turbulent Separated Flow," AGARD-AG-287, Vol. 1, June 1985.

[2]Bradbury, L. J. S., and Castro, I. P., "A Pulsed-Wire Technique for Velocity Measurement in Highly Turbulent Flow," *Journal of Fluid Mechanics*, Vol. 49, Pt. 4, 1971, pp. 657–692.

[3]Coles, D., and Wadcock, A. J., "A Flying Hotwire Study of Two-Dimensional Mean Flow Past an NACA 4412 Airfoil at Maximum Lift," *AIAA Journal*, Vol. 17, No. 4, 1979, pp. 321–329.

[4]Nakayama, A., "Application of Split-Film Probe to Measurement of Flows with High Turbulence Intensity," AIAA Paper 91-064, Jan. 1991.

[5]Modera, M. P., "Periodic Flow Through Thin-Plate Slots," Doctoral Dissertation, Dept. of Heating and Ventilating, Royal Inst. of Technology, Stockholm, Sweden, 1989.

[6]Doiron, M. D., "Attached and Separated Trailing Edge Flow Measurements with a Triple-Split Hot-Film Probe," M.A.Sc. Thesis, Institute for Aerospace Studies, Univ. of Toronto, Toronto, Canada, Oct. 1992.

[7]Jørgensen, F. E., "Characteristics and Calibration of a Triple-Split Probe for Reversing Flows," *DISA Information*, No. 27, Jan. 1982, pp. 15–22.

[8]Shook, M., Stock, D. E., and Bowen, A. J., "Split-Film Anemometry," 1990 Spring Meeting of the Fluids Engineering Div., American Society of Mechanical Engineers, 1990.

[9]Pulliam, T. H., "Efficient Solution Methods for the Navier-Stokes Equations," Lecture Notes for the Von Kármán Institute for Fluid Dynamics Lecture Series, *Numerical Techniques for Viscous Flow Computation in Turbomachinery Bladings*, Von Kármán Inst. for Fluid Dynamics, Brussels, Belgium, Jan. 1986.

[10]Nelson, T. E., Zingg, D. W., and Johnston, G. W., "Compressible Navier-Stokes Computations of Multielement Airfoil Flows Using Multiblock Grids," *AIAA Journal*, Vol. 32, No. 3, 1994, pp. 506–511.

Nonlinear Thermal Dynamic Analysis of Graphite/Aluminum Composite Plates

R. Tenneti* and K. Chandrashekhara†
University of Missouri–Rolla, Rolla, Missouri 65401

Introduction

BECAUSE of the increased application of composite materials in high-temperature environments, the thermoelastic analysis of laminated composite structures is important. Many researchers have applied the classical lamination theory to analyze laminated plates under thermomechanical loading,[1] which neglects shear deformation effects. The transverse shear deformation effects are not negligible as the ratios of inplane elastic modulus to transverse shear modulus are relatively large for fiber-reinforced composite laminates. The application of first-order shear deformation theory for the thermoelastic analysis of laminated plates has been reported by only a few investigators.[2–4] Reddy and Hsu[2] have considered the thermal bending of laminated plates. The analytical and finite element solutions for the thermal buckling of laminated plates have been reported by Tauchert[3] and Chandrashekhara,[4] respectively. However, the first-order shear deformation theory, based on the assumption of constant distribution of transverse shear through the thickness, requires a shear correction factor to account for the parabolic shear strain distribution. Higher order theories have been proposed which eliminate the need for a shear correction factor.[5] In the present work, nonlinear dynamic analysis of laminated plates subjected to rapid heating is investigated using a higher order shear deformation theory. A C^0 finite element model with seven degrees of freedom per node is implemented and numerical results are presented for laminated graphite/aluminum plates.

Mathematical Formulation

A laminated composite plate having length a, width b, and thickness h is considered. The higher order displacement field assumed can be expressed as

$$\begin{aligned} u(x, y, z, t) &= u_0(x, y, t) + z\psi_x(x, y, t) + z^3\phi_x(x, y, t) \\ v(x, y, z, t) &= v_0(x, y, t) + z\psi_y(x, y, t) + z^3\phi_y(x, y, t) \\ w(x, y, z, t) &= w_0(x, y, t) \end{aligned} \quad (1)$$

Received June 26, 1993; revision received Jan. 22, 1994; accepted for publication Feb. 5, 1994.

*Graduate Research Assistant; currently at EGS, Inc., Oak Park, MI 48237.

†Associate Professor, Department of Mechanical and Aerospace Engineering and Engineering Mechanics. Member AIAA.